Secondary-electron emission from specularly reflected MeV protons

Kenji Kimura,* Suguru Ooki, Gou Andou, Kaoru Nakajima, and Michi-hiko Mannami
Department of Engineering Physics and Mechanics, Kyoto University, Kyoto 606-8501, Japan
(Received 26 February 1998)

Secondary-electron yield induced by MeV protons specularly reflected from a SnTe(001) surface is measured. From the observed secondary-electron yield, the position-dependent secondary-electron production rate $P(x)$ is derived as a function of distance x from the surface. The obtained $P(x)$ can be explained in terms of the direct electron excitation as well as the decay of both bulk and surface plasmons excited by the proton. The probability of surface plasmon decay to an electron-hole pair is estimated to be ~30%.
[S1050-2947(98)00708-2]

PACS number(s): 34.50.Dy, 79.20.Rf

I. INTRODUCTION

Since the discovery by Villard in 1899 [1], ion-induced electron emission from solids has been studied for a long time [2]. There are two different mechanisms of the electron emission under bombardment of ions. When the potential energy of the projectile is larger than twice the work function of the target material, potential emission may occur at the surface [3]. Recently, this phenomenon has been extensively studied with highly charged ions [4]. If the target electrons are excited by direct transfer of kinetic energy from the projectile, these electrons may appear outside the target as secondary electrons. This process, called kinetic electron emission, is usually dominant for ion velocity larger than about 10^7 cm/s [5]. The mechanism of the kinetic electron emission is explained by a so-called three-step model [6]: generation of excited electrons in the solid, transportation to the surface, transmission through the surface barrier. In theoretical studies, these processes are assumed to be independent and are analyzed separately. Even for one of these processes, however, a complete treatment is an immense task and some simplifications are usually introduced. The generation process, for example, contains direct excitation of valence and inner-shell electrons by primary ions, one-electron decay of bulk and surface plasmons generated by primary ions, Auger electron emission, etc. The generation rate is usually assumed to be proportional to the inelastic stopping power instead of the complete treatment. This assumption is thought to be justified by the observed proportionality between the secondary electron yield and the stopping power. However, the observed proportionality does not directly guarantee the assumption because the observed secondary electron yield is a result of these complicated processes, i.e., generation, transportation, and transmission. If the generation process can be observed separately from other processes, applicability of the assumption can be clear.

When a fast ion is incident on a single-crystal surface with a grazing angle, the ion is reflected from the surface without penetration inside the crystal if the angle θ_i of incidence from the surface plane is smaller than a critical angle [7,8]. The ion may excite target electrons outside the crystal. These electrons can be directly emitted to vacuum without other processes. This allows us to study the generation process separately from others. In this paper, we report on the measurement of the secondary-electron yield induced by specularly reflected MeV protons. Analyzing the results, detailed information on the generation process is obtained.

II. EXPERIMENTAL PROCEDURE

A single crystal of SnTe(001) was prepared by epitaxial growth *in situ* by vacuum evaporation on a cleaved surface of KCl at 250 °C in a UHV chamber. The crystal was mounted on a five-axis precision goniometer. Beams of 0.5–1.5 MeV protons from the 1.7-MV Tandetron accelerator of Kyoto University were incident on the crystal at glancing angles $\theta_i = 2-7$ mrad. The beams were collimated by a series of apertures to less than 0.1×0.1 mm^2 and to a divergence angle less than 0.3 mrad. The azimuthal angle of the crystal was carefully chosen to avoid surface axial channeling. The protons scattered at a specular angle were selected by an aperture ($\phi = 1$ mm) placed 425 mm downstream from the target and energy analyzed by a 90° sector magnetic spectrometer.

The observed energy spectrum of 0.5 MeV protons reflected from the SnTe(001) is shown in Fig. 1. Besides a main peak at ~496.5 keV, which corresponds to the specularly reflected protons and is referred to as the first peak hereafter, there are additional small peaks at ~489.5 and ~483 keV. These small peaks, being referred to as the second and third peaks, correspond to the protons which penetrated through side surfaces of surface steps and appeared again after channeling through the crystal as shown in the inset [9]. The energy loss of the second peak proton is about three times as large as that of the first peak proton because the second peak proton is deflected by the atomic plane three times while the first peak proton is deflected once.

Secondary electrons emitted from the target crystal were detected by a microchannel plate (MCP, effective diameter $\phi = 20$ mm) placed in front of the target. The distance between the crystal surface and the MCP was 12.5 mm and the dimension of the crystal surface along the beam direction was about 7 mm. The MCP was biased at +500 V to collect all secondary electrons emitted from the target. Although the

*Author to whom correspondence should be addressed. FAX: +81-75-753-5253. Electronic address: kimura@kues.kyoto-u.ac.jp

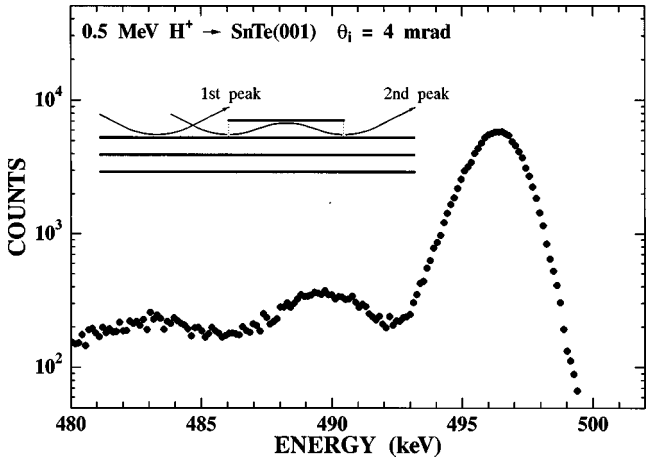

FIG. 1. Energy spectrum of protons specularly reflected from a SnTe(001) surface when 0.5-MeV protons are incident on the surface at $\theta_i = 4$ mrad. The first peak at ~496.5 keV corresponds to the protons reflected without penetration into the crystal and small peaks at ~490 and 483 keV correspond to subsurface channeled ions as shown by the inset.

applied bias affected the proton trajectory, the deflection caused by the bias of 500 V was less than 0.2 mrad for the 0.5-MeV proton.

III. EXPERIMENTAL RESULT

Figure 2 displays an example of the pulse height distribution of MCP signal (solid circles) measured in coincidence with the first peak proton when 0.5-MeV protons were incident on the SnTe(001) at $\theta_i = 4$ mrad. The pulse height I of the MCP signal is proportional to the number of secondary electrons detected. [10] In order to derive the number of secondary electrons emitted by one proton from the observed pulse height distribution, we need the pulse height of the MCP signal for single-electron detection. The open circles show the result without the proton beam. There were many free electrons inside the chamber, which mainly came from

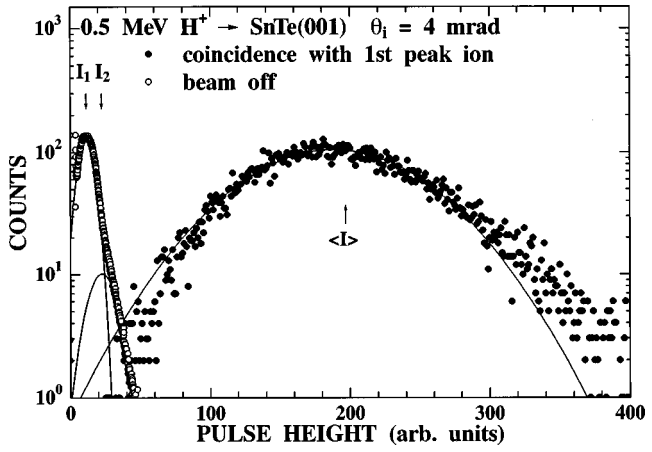

FIG. 2. Pulse height distribution of secondary electrons detected by MCP in coincidence with the reflected protons of the first peak when 0.5-MeV protons are incident on the SnTe(001) at $\theta_i = 4$ mrad. The open circles show pulse height distribution measured without the proton beam, which corresponds to signals of single-electron detection.

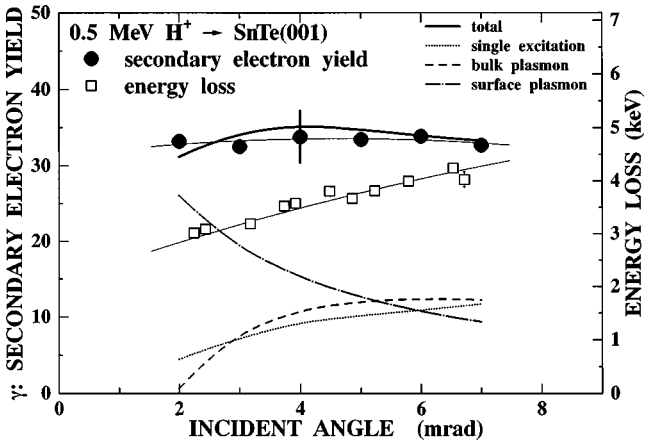

FIG. 3. Secondary-electron yield induced by 0.5-MeV protons specularly reflected from a SnTe(001) as a function of the angle of incidence (●). The energy loss of the specularly reflected 0.5-MeV proton (□) is also shown. Calculated contributions to the secondary-electron yield for single-electron excitation (dotted curve), bulk plasmon decay (dashed curve), and surface plasmon decay (dot-and-dashed curve) as well as the sum of them (solid curve) are shown. A typical experimental error is also shown.

an ion pump used to evacuate the chamber. The pulse height distribution observed without the proton beam is attributed to these free electrons and it can be decomposed into two Gaussians as shown in Fig. 2. The peak positions I_1 and I_2 of the Gaussians have a relation $I_2 = 2I_1$ indicating that these Gaussians correspond to signals of single- and double-electron detections. The secondary electron yield, i.e., a mean number of the secondary electrons emitted by single proton, can be estimated by $\gamma = \langle I \rangle / (\varepsilon I_1)$, where $\langle I \rangle$ denotes the mean value of the pulse height distribution, and ε is the detection efficiency of MCP, which was measured to be 0.6 for 0.5-keV electrons [11]. The obtained secondary electron yield for the 0.5-MeV proton is shown in Fig. 3 as a function of the angle of incidence together with the energy losses ΔE observed in a previous study [12]. While the energy loss increases with θ_i, the secondary electron yield is almost constant. Figure 4 shows the observed secondary electron yield as a function of ion energy at $\theta_i = 5$ mrad. Energy losses of reflected protons measured in a previous study [13] are also shown for comparison. Although the secondary-electron yield decreases with increasing energy, the energy loss is almost constant.

IV. POSITION-DEPENDENT SECONDARY ELECTRON PRODUCTION RATE

The secondary electron yield is written as

$$\gamma(\theta_i) = \int_{\text{traj}} P(x)\,dz, \tag{1}$$

where $P(x)$ is a position-dependent secondary-electron production rate, i.e., the number of secondary electrons produced by a proton per unit path length traveling parallel to the surface at a distance x from the surface and the integral is performed along the proton trajectory that lies in the x-z

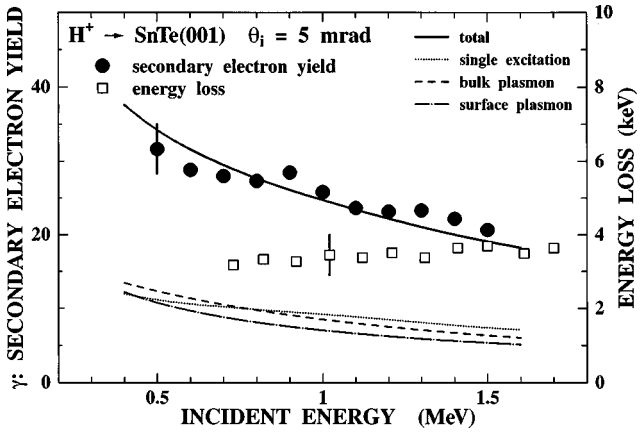

FIG. 4. Secondary-electron yield induced by protons specularly reflected from a SnTe(001) surface ($\theta_i = 5$ mrad) as a function of the proton energy. The energy loss of the reflected proton measured in a previous paper [13] is shown for comparison (□). Calculated contributions for single electron excitation (dotted curve), bulk plasmon decay (dashed curve), and surface plasmon decay (dot-and-dashed curve) as well as the sum of them (solid curve) are shown. A typical experimental error is also shown.

plane. Using the surface continuum potential $V(x)$ the trajectory can be calculated and Eq. (1) is written as

$$\gamma(\theta_i) = 2\sqrt{E}\int_{x_m(\theta_i)}^{+\infty} \frac{P(x)}{\sqrt{V(x_m(\theta_i)) - V(x)}}\, dx, \qquad (2)$$

where E is the proton energy and $x_m(\theta_i)$ is the closest approach to the surface. This is an integral equation of Abel type and the solution is given by

$$P(x) = -\frac{1}{2\pi E}\frac{dV(x)}{dx} \times \left(\gamma(0)\sqrt{\frac{E}{V(x)}} + \int_0^{\pi/2} \left.\frac{d\gamma(\theta_i)}{d\theta_i}\right|_{\theta_i = \sqrt{\frac{V(x)}{E}}\sin(u)} du \right). \qquad (3)$$

Thus, the production rate can be derived from the observed $\gamma(\theta_i)$. This procedure is essentially the same as that used for derivation of position-dependent stopping power [14].

Figure 5 shows the obtained production rate for the 0.5-MeV proton. In the calculation of Eq. (3), the Moliére potential was employed for $V(x)$ and the experimental $\gamma(\theta_i)$ was approximated by a quadratic function as shown by a thin solid curve in Fig. 3. The position-dependent stopping power $S(x)$ for the 0.5-MeV proton can be also derived from the observed energy loss using a similar equation to Eq. (3) [replacing $P(x)$ and $\gamma(\theta_i)$ with $S(x)$ and $\Delta E(\theta_i)$]. The result is shown by a dotted line in Fig. 5. Both the secondary-electron production rate and the stopping power decrease exponentially with x, but stopping power decreases more rapidly.

V. DISCUSSION

In a phenomenological theory of the kinetic electron emission, the secondary-electron generation rate is assumed to be proportional to the stopping power [6]. However, the

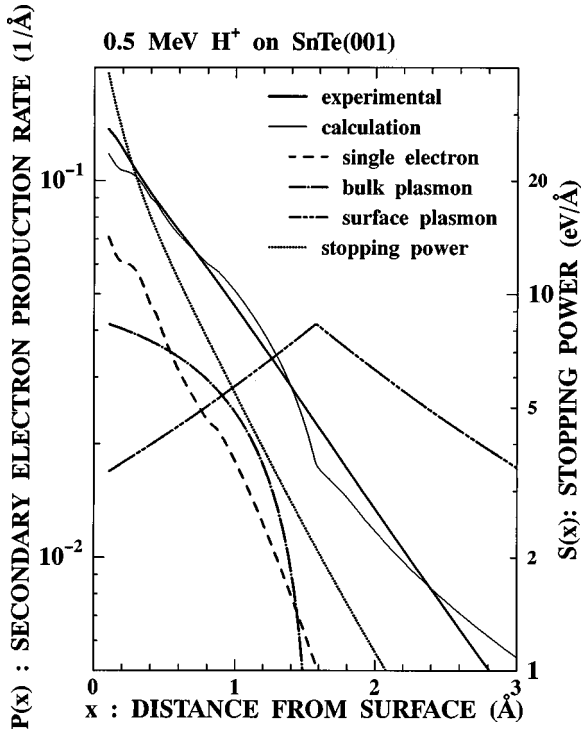

FIG. 5. Secondary-electron production rate for the 0.5-MeV proton as a function of distance from the surface derived from the measured $\gamma(\theta_i)$ (thick solid curve). Calculated results with a simple model (see the text) are also shown. Position-dependent stopping power is shown for comparison (dotted curve).

present result indicates that this proportionality does not hold. The ratio $S(x)/P(x)$ depends on the distance from the surface as can be seen in Fig. 5, e.g., the ratio is about 160 eV/electron at $x = 0.5$ Å and 80 eV/electron at $x = 2$ Å. This means that the proton traveling at large x emits electrons more efficiently than that at small x. Detailed consideration of the excitation process is needed to understand the present result. Although there have been several theoretical studies about secondary-electron emission by glancing angle scattering of fast ions [15,16], they concentrated on the calculation of the energy and angular distributions of secondary electrons. Neither the position-dependent production rate nor the total secondary-electron yield by a specularly reflected ion was given. Here, the position-dependent production rate is estimated with a simple model.

The number of electrons excited over the vacuum level per unit path length of the proton at x can be calculated with a binary encounter model,

$$P_{\mathrm{s.c.}}(x) = \frac{2\pi e^4}{m\nu^2}\sum_i n_i(x)\left(\frac{1}{\varepsilon_i} - \frac{1}{2m\nu^2}\right), \qquad (4)$$

where m is the electron mass, $n_i(x)$ is the electron density of the ith shell averaged over the plane parallel to the surface and ε_i is its binding energy. Hartree-Fock wave functions [17] of isolated Sn and Te atoms were used to calculate $n_i(x)$. It is reasonable to assume that half of these excited electrons are ejected to the vacuum and others impinge into the solid. Therefore, the calculated result, $P_{\mathrm{s.c.}}(x)/2$, for the 0.5-MeV proton is compared with the experimental result in Fig. 5 (dashed curve). The calculated result reproduces nei-

ther the absolute value nor the x dependence of the experimental result. The calculated production rate is smaller and decreases more rapidly with distance from the surface. This discrepancy might be attributed to the secondary electrons created by plasmon decay. The role of plasmon decay on secondary electron emission was first pointed out by Gornyi [18] and evidence of the plasmon decay was found in the energy spectra [19].

The plasmon excitation rate by fast ions traveling near the surface was calculated by Kawai, Itoh, and Ohtsuki [20]. The calculated results for both bulk and surface plasmons are shown in Fig. 5 (dot-and-dashed and double-dot-and-dashed curves). As the half of the free electrons created by the plasmon decay are expected to be ejected to the vacuum, the halves of the calculated plasmon excitation rates are shown. In the calculation, the electronic surface was assumed to be outside of the atomic surface by half of the interplanar separation (3.15 Å/2) and the bulk plasmon energy of 15 eV was employed. While almost all bulk plasmons decay into electron-hole pairs, surface plasmons can decay via photon emission [21]. The fraction F of the surface plasmons that create electron-hole pairs depends on the surface conditions [22]. The total secondary-electron production rate $P(x)$ calculated with various F values was compared with the experimental one. The best fit between the calculated and experimental results was obtained with $F=0.3$ as shown in Fig. 5 (thin solid curve). The probability of surface plasmon decay into an electron-hole pair was measured to be 0.3 for Al films with smooth surfaces [22]. The present result coincides with this value.

The secondary-electron yield was calculated by integration of the theoretical $P(x)$ along the trajectory and the results are shown in Figs. 3 and 4. The agreement between the calculated and experimental results is reasonably good. It should be noted that the contribution from the surface plasmon decay is dominant at small θ_i (see Fig. 3). This is very different from the case of normal incidence. The role of plasmon decay on secondary electron emission was discussed by Chung and Everhart for the case of normal incidence of keV electrons on nearly-free-electron metals [23]. They found that the contribution of the surface plasmon decay is negligibly small.

It is known that the secondary-electron yield from a single crystal has minima under channeling conditions [24–26]. This was explained by the fact that the electronic stopping power for channeled ions is smaller than that for the ions of random incidence. Assuming that the excitation probability is proportional to the position-dependent stopping power, the secondary electron yield for a channeled ion was analyzed and an effective mean escape length was estimated [26]. The present result, however, indicates that this assumption is not correct. Detailed analysis is needed to understand the effect of channeling on the secondary-electron emission.

VI. CONCLUSION

We have demonstrated that the position-dependent secondary-electron production rate can be derived from the secondary-electron yield observed at glancing angle scattering of fast protons from a single-crystal surface. The obtained production rate decreases less rapidly than the position-dependent stopping power with increasing distance from the surface. This indicates that the proportionality between the stopping power and the electron production rate, which has been assumed in many phenomenological theories of the secondary electron emission, does not hold. The obtained position-dependent secondary electron production rate can be explained by a simple model, which takes account of both the single-electron excitation and the electron-hole pair creation by plasmon decay, with a suitable choice of a fitting parameter.

ACKNOWLEDGMENTS

We are grateful to the members of the Department of Nuclear Engineering at Kyoto University for the use of the Tandetron accelerator, and to Professor M. Rösler for fruitful discussions.

[1] M. P. Villard, J. Phys. Theor. Appl. Ser. **8**, 5 (1899).

[2] See, for example, M. Rösler and W. Brauer, in *Particle Induced Electron Emission I*, edited by G. Hohler and E. A. Niekisch, Springer Tracts in Modern Physics, Vol. 122 (Springer, Heidelberg, 1991), p. 1.

[3] H. D. Hagstrum, in *Inelastic Ion-Surface Collisions*, edited by N. H. Tolk *et al.* (Academic, New York, 1977), p. 1.

[4] J. W. McDonald, D. Schneider, M. W. Clark, and D. Dewitt, Phys. Rev. Lett. **68**, 2297 (1992); F. Aumayr, H. Kutz, D. Schneider, M. A. Briere, J. W. McDonald, C. E. Cunningham, and HP Winter, *ibid.* **71**, 1943 (1993).

[5] R. A. Baragiola, E. V. Alonso, J. Ferron, and A. Oliva-Florio, Surf. Sci. **90**, 240 (1979).

[6] See, for example, D. Hasselkamp, in *Particle Induced Electron Emission II*, edited by G. Hohler and E. A. Niekisch, Springer Tracts in Modern Physics, Vol. 123 (Springer, Heidelberg, 1991), p. 1.

[7] G. S. Harbinson, B. W. Farmery, H. J. Pabst, and M. W. Thompson, Radiat. Eff. **27**, 97 (1975).

[8] M. Mannami, K. Kimura, K. Nakanishi, and A. Nishimura, Nucl. Instrum. Methods Phys. Res. B **13**, 587 (1986).

[9] K. Kimura, M. Hasegawa, Y. Fujii, M. Suzuki, Y. Susuki, and M. Mannami, Nucl. Instrum. Methods Phys. Res. B **33**, 358 (1988).

[10] B. Monart, Ph.D. thesis, Paris Sud University, 1988, IPNO-T-88-01.

[11] M. Galanti, R. Gott, and J. F. Renaud, Rev. Sci. Instrum. **42**, 818 (1971).

[12] K. Kimura, H. Kuroda, M. Fritz, and M. Mannami, Nucl. Instrum. Methods Phys. Res. B **100**, 356 (1995).

[13] Y. Fujii, S. Fujiwara, K. Narumi, K. Kimura, and M. Mannami, Surf. Sci. **277**, 164 (1992).

[14] K. Kimura, M. Hasegawa, and M. Mannami, Phys. Rev. B **36**, 7 (1987).

[15] D. L. Mills, Surf. Sci. **294**, 161 (1993).
[16] F. J. Garcia de Abajo and P. M. Echenique, Nucl. Instrum. Methods Phys. Res. B **79**, 15 (1993).
[17] H. Herman and S. Skilman, *Atomic Structure Calculations* (Prentice-Hall, Englewood Cliffs, NJ, 1963).
[18] N. B. Gornyi, Fiz. Tverd. Tela **8**, 1939 (1966) [Sov. Phys. Solid State **8**, 1535 (1966)].
[19] N. B. Gornyi, L. M. Rakhovich, and S. F. Skirko, Izv. Vyssh. Uchebn. Zaved. Fiz. **10**, 19 (1967) [Sov. Phys. J. **10**, 15 (1967)].
[20] R. Kawai, N. Itoh, and Y. H. Ohtsuki, Surf. Sci. **114**, 137 (1982).
[21] H. Raether, in *Surface Plasmons on Smooth and Rough Surfaces and on Gratings*, Springer Tracts in Modern Physics, Vol. 111 (Springer, Heidelberg, 1988).
[22] J. C. Endritz and W. E. Spicer, Phys. Rev. B **4**, 4159 (1971).
[23] M. S. Chung and T. E. Everhart, Phys. Rev. B **15**, 4699 (1977).
[24] E. S. Mashkova, V. A. Molchanov, and D. d. Odintsov, Dokl. Akad. Nauk. SSSR **151**, 1074 (1963) [Sov. Phys. Dokl. **8**, 806 (1963)].
[25] N. Benazeth, Nucl. Instrum. Methods **194**, 405 (1982).
[26] M. Hasegawa, T. Fukuchi, Y. Susuki, S. Fukui, K. Kimura, and M. Mannami, Jpn. J. Appl. Phys., Part 1 **30**, 2074 (1991).